Viscous control of shallow elastic fracture

Tim Large[1], John Lister[2], and Dominic Skinner[2]

[1]Massachusetts Institute of Technology, USA

[2]Department of Applied Mathematics and Theoretical Physics, University of Cambridge, UK

(Received 30 October 2016; revised xx; accepted xx)

This paper considers the problem of a semi-infinite crack parallel to the boundary of a half plane, with the crack filled by an incompressible viscous fluid. The dynamics are driven by a bending moment applied to the arm of the crack, and we look for travelling wave solutions. We examine two models of fracture; fracture with a single tip, and fracture with a wet tip proceded by a region of dry fracture.

Key words: Authors should not enter keywords on the manuscript, as these must be chosen by the author during the online submission process and will then be added during the typesetting process (see http://journals.cambridge.org/data/ relatedlink/jfm-keywords.pdf for the full list)

1. Introduction

Consider a semi infinite elastic solid, with a thin strip peeled off, and the resulting crack filled with an incompressible fluid with viscosity μ, as shown in figure 1. The motion is driven by a constant bending moment M. We look for travelling wave solutions, propagating with speed c. We define the origin to be instantaneously at the crack tip, and the positive x axis to be aligned in the direction of the crack. We define the vertical displacement to be $h(x)$, the horizontal displacement to be $g(x)$, and the thickness of the strip as l.

We consider the case of a slowly propagating crack where inertia becomes negligible. In addition, near the crack tip, the crack considered is long and thin, and as such, the flow is assumed to be in lubrication everywhere. The fracture is assumed to obey linear elastic fracture mechanics, which describes well the fracture of brittle solids. Since we have posed a two dimensional problem, only mode I and mode II fractures are of relevance. These are governed by two fracture toughness constants K_I, K_{II}. This paper will calculate the speed of travelling waves c for any combination of K_I, K_{II}. To do that, we also consider a geometry where the mode II fracture preceeds the fluid tip.

The problem considered here is relevant to the physical problem of the expansion of a magma bubble just under the surface, with the motion being driven by a flux of magma into the bubble. Consider just the outer edges of such an expanding bubble. Looking at just the crack tip, the problem becomes the one studied in this paper, where the motion is driven by some far off bending moment.

The dry, static problem of a semi-infinite crack parallel to a half space has been studied by Zlatin & Khrapkov (1986). A related problem of a finite length crack in an elastic solid has been studied by Thouless et al. (1987). Dyskin et al. (2000) have considered a finite length crack below a free surface in a semi-infinite solid. The problem of fluid

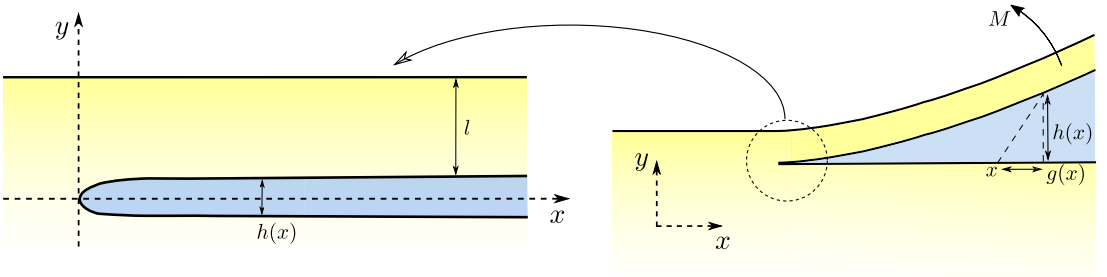

FIGURE 1. A picture of the geometry of the problem. On the left is a close up of the crack tip, while on the right is the geometry for large x.

driven fracture in a penny shaped crack, driven by a source inlet has been studied by Garagash & Detournay (2005).

2. Formulation of problem

2.1. *Single tip*

From lubrication, we have Poiseulle flow in the crack. We obtain the flux, and conservation of mass as

$$q = -\frac{1}{12\mu}\frac{\mathrm{d}p}{\mathrm{d}x}h^3\,, \qquad \frac{\partial q}{\partial x} + \frac{\partial h}{\partial t} = 0\,, \tag{2.1}$$

from which, the pressure is found to be

$$p(x) = -\int_x^\infty 12\mu c/h(\tilde{x})^2 \mathrm{d}\tilde{x}\,. \tag{2.2}$$

From (citations to relevant papers) who have studied an elastic solid with the same geometry, we have

$$\begin{bmatrix} -\sigma_y \\ -\tau_{xy} \end{bmatrix} = \begin{bmatrix} p(x) \\ 0 \end{bmatrix} = \frac{E}{4\pi l(1-\nu^2)}\int_0^\infty \boldsymbol{K}\left(\frac{\tilde{x}-x}{l}\right)\begin{bmatrix} g'(\tilde{x}) \\ h'(\tilde{x}) \end{bmatrix}\mathrm{d}\tilde{x}\,, \tag{2.3}$$

where the integral kernel is

$$\boldsymbol{K}(\xi) = \begin{bmatrix} K_{11} & K_{12} \\ K_{21} & K_{22} \end{bmatrix} = \begin{bmatrix} \frac{(32-24\xi^2)}{(\xi^2+4)^3} & \frac{(48\xi^2-64)}{\xi(\xi^2+4)^3} \\ -\frac{(16\xi^4+16\xi^2+4)}{\xi(\xi^2+4)^3} & -\frac{(32-24\xi^2)}{(\xi^2+4)^3} \end{bmatrix}. \tag{2.4}$$

The boundary conditions near $x = 0$ are governed by fracture mechanics,

$$K_I \geqslant \lim_{x\to 0}\frac{E}{1-\nu^2}\sqrt{\frac{\pi}{8}}\sqrt{x}\,h'(x)\,, \qquad K_{II} \geqslant \lim_{x\to 0}\frac{E}{1-\nu^2}\sqrt{\frac{\pi}{8}}\sqrt{x}\,g'(x)\,. \tag{2.5a, b}$$

Where equality holds in at least one of the two equations.

Considering the region $x \gg l$, the problem becomes a question of peeling off a thin strip from an elastic half space. The elasticity equations can then be simplified by modelling the strip using beam theory. This gives the equations

$$M(x) = \frac{El^3}{12(1-\nu^2)}\frac{\mathrm{d}^2 h}{\mathrm{d}x^2} = \frac{El^2}{6(1-\nu^2)}\frac{\mathrm{d}g}{\mathrm{d}x}, \qquad p = \frac{El^3}{12(1-\nu^2)}h^{(4)}(x) \tag{2.6a, b}$$

As $x \to \infty$, $M(x) \to M$, the applied bending moment, therefore these equations provide boundary conditions on h'', g'.

2.2. *Double tip*

Consider the mode II fracture preceeding the fluid tip at $x = 0$ by a distance lL, so $h(x), h'(x) = 0$ for $-lL < x < 0$ (but $g \neq 0$). Since the solid has already fractured, $h'(x)$ does not have an $x^{-1/2}$ singularity at $x = 0$. The boundary conditions at the crack tip become

$$\lim_{x\to 0} \sqrt{x}\, h'(x) = 0\,, \qquad \lim_{x\to -Ll} \frac{E}{1-\nu^2}\sqrt{\frac{\pi}{8}}\sqrt{x}\, g'(x) \;= K_{II}. \tag{2.7a, b}$$

2.3. *Rescaling*

We can define the following dimensionless variables

$$x = l\xi, \quad h(x) = \frac{12M(1-\nu^2)}{El} H(\xi), \quad g(x) = \frac{12M(1-\nu^2)}{El} G(\xi)\,, \tag{2.8}$$

$$p = \frac{3M}{\pi l^2}\Pi(\xi), \quad K_I = Ml^{-3/2}\kappa_I, \quad K_{II} = Ml^{-3/2}\kappa_{II}, \quad \lambda = \frac{4\pi\mu p^* l^3}{M^2}\,. \tag{2.9}$$

With these scalings, the equations become

$$\begin{bmatrix} \Pi \\ 0 \end{bmatrix} = \int_0^\infty \boldsymbol{K}(\tilde{\xi} - \xi) \begin{bmatrix} G'(\tilde{\xi}) \\ H'(\tilde{\xi}) \end{bmatrix} \mathrm{d}\tilde{\xi} \tag{2.10}$$

$$H^2 \frac{\mathrm{d}\Pi}{\mathrm{d}\xi} = \lambda \quad \text{or} \quad \Pi(\xi) = -\int_\xi^\infty \lambda / H(\tilde{\xi})^2 \mathrm{d}\tilde{\xi} \tag{2.11a, b}$$

$$\lim_{\xi\to\infty} H'' = 1, \quad \lim_{\xi\to\infty} G' = \frac{1}{2}, \quad \lim_{\xi\to 0} 3\sqrt{2\pi\xi} H' \leqslant \kappa_I, \quad \lim_{\xi\to 0} 3\sqrt{2\pi\xi} G' \leqslant \kappa_{II}, \tag{2.12}$$

These shall be the governing equations for the rest of this paper.

2.4. *Beam theory asymptotics*

In the dimensionless variables, the outer asymptotics are of the form

$$\frac{\mathrm{d}^2 H}{\mathrm{d}\xi^2} = \frac{1}{2}\frac{\mathrm{d}G}{\mathrm{d}\xi}, \qquad H^{(4)}(\xi) = \frac{3}{\pi}\Pi(\xi), \qquad \frac{\mathrm{d}^2 H}{\mathrm{d}\xi^2} \to 1 \tag{2.12a, b, c}$$

From integration by parts, we can write

$$H''(\xi) = 1 - \frac{1}{2}\int_\xi^\infty (\tilde{\xi} - \xi)^2 H^{(5)}(\tilde{\xi}) \mathrm{d}\tilde{\xi}, \tag{2.13}$$

then using equation 2.11a, it is found that

$$H''(\xi) = 1 - \frac{3\lambda}{2\pi}\int_\xi^\infty \frac{(\tilde{\xi} - \xi)^2}{H(\tilde{\xi})^2} \mathrm{d}\tilde{\xi}. \tag{2.14}$$

But we know $H(\xi) = \frac{1}{2}\xi^2 + o(\xi^2)$, as $\xi \to \infty$, and so we use this to get a better estimate of H'';

$$H''(\xi) = 1 - \frac{2\lambda}{\pi}\frac{1}{\xi} + o(1/\xi). \tag{2.15}$$

This new expression can be used to refine the error estimate from $o(1/\xi)$, to $O(\log(\xi)/\xi^2)$.

3. Numerical scheme

3.1. *Single Tip*

We discretize the problem by taking $n+1$ points $\boldsymbol{\xi} = (\xi_0 = 0, \xi_1 \ldots, \xi_n)$ at which we measure H', G', and n intermediate points $\boldsymbol{\zeta} = (\zeta_0, \ldots, \zeta_{n-1})$ at which to measure Π, so that $\xi_0 < \zeta_0 < \ldots < \zeta_{n-1} < \xi_n$. We work with $\sqrt{\xi}G'(\xi)$, $\sqrt{\xi}H'(\xi)$ near the tip to avoid singularities. We define $\boldsymbol{\theta}_G = [\sqrt{\xi_0}G'(\xi_0), \ldots, \sqrt{\xi_{t-1}}G'(\xi_{t-1}), G'(\xi_t), \ldots G'(\xi_n)]$, and $\boldsymbol{\theta}_H$ similarly, as well as $\boldsymbol{\theta} = [\boldsymbol{\theta}_G, \boldsymbol{\theta}_H]$, Typically $t \approx n/2$ was used. From the linearity of the elasticity integral (and the discretized integral) we may write

$$[\Pi(\zeta_1), \ldots, \Pi(\zeta_{n-1}), \underbrace{0, \ldots, 0}_{n-1}] = \boldsymbol{J}\boldsymbol{\theta}\,, \tag{3.1}$$

for some matrix $\boldsymbol{J}$. One can recover $H(\xi_i)$ from $\boldsymbol{\theta}_H$. Therefore, a discritized lubrication integral, yields an expression for $\Pi(\zeta_i)$ as a function of $\boldsymbol{\theta}_H$. So we can write

$$[\Pi(\zeta_1), \ldots, \Pi(\zeta_{n-1}), \underbrace{0, \ldots, 0}_{n-1}] = \boldsymbol{J}\boldsymbol{\theta} = \boldsymbol{f}(\boldsymbol{\theta}_H)\,, \tag{3.2}$$

for some function $\boldsymbol{f}$.

The values of both $G'(\xi_n)$, and $H''(\xi_n)$ are known from our beam theory asymptotic expansion. But these are linear in $\boldsymbol{\theta}$, since $G'(\xi_n) = \theta_n$, and $H''(\xi_n) \approx (\theta_{2n} - \theta_{2n-1})/(\xi_n - \xi_{n-1})$, Therefore we can add another two rows to $\boldsymbol{J}$, so that

$$\boldsymbol{A}\boldsymbol{\theta} = [\boldsymbol{f}(\boldsymbol{\theta}), G'(\xi_n), H''(\xi_n)]\ . \tag{3.3}$$

Where the $\boldsymbol{A}$ is the enlarged matrix. This can be solved by Newton's method from quite arbitrary initial guesses.

For $\xi_i < \xi < \xi_{i+1}$, we interpolate as

$$G'(\xi) = \begin{cases} \xi^{-1/2}(a_i\xi + b_i) \\ a_i\xi + b_i \end{cases}, \quad H'(\xi) = \begin{cases} \xi^{-1/2}(c_i\xi^{1/2} + d_i) \\ c_i\xi + d_i \end{cases}, \quad \text{for} \quad \begin{cases} i < t \\ i \geqslant t \end{cases} \tag{3.4}$$

The choice of interpolating function was based on the appearance of the relevant functions. We will also define a_n, b_n, c_n, d_n for interpolation beyond ξ_n. With this choice of interpolation, there exist exact closed form expressions for both the lubrication integral, and the elasticity integral, in terms of the $a_i - d_i$ coefficients.

It therefore remains to determine $a_i - d_i$ in terms of $\boldsymbol{\theta}$. Continuity of G', H' imposes $2(n-1)$ linear equations. We also have the $2n$ equations following from the definition of $\boldsymbol{\theta}$, (such as $a_i\xi_i + b_i = \theta_i$ for $t \leqslant i \leqslant n$).

From our asymptotic expansion (via beam theory) we know $\theta_n = G'(\xi_n)$ and $a_n = G''(\xi_n)$. Therefore we can write

$$a_n = \frac{G''(\xi_n)}{G'(\xi_n)}\theta_n, \qquad b_n = \theta_n - a_n\xi_n = \left(1 - \frac{G''(\xi_n)}{G'(\xi_n)}\xi_n\right)\theta_n. \tag{3.5}$$

With H, we know that $c_n = H''(\xi_n)$, $c_{n-1} = H''(\xi_{n-1})$, and so we have that

$$c_n = \frac{H''(\xi_n)}{H''(\xi_{n-1})}c_{n-1}, \qquad d_n = -c_n\xi_n + c_{n-1}\xi_n + d_{n-1}. \tag{3.6}$$

Therefore, we have enough equations to know the $a_i - d_i$ in terms of $\boldsymbol{\theta}$.

Note that numerically, we choose a value of λ, solve the problem and subsequently recover the boundary conditions at $\xi = 0$ (κ_I, κ_{II}). This can then be inverted, so that we think of $\lambda = \lambda(\kappa_I)$, since this is the physical interpretation.

The spacing of the points should reflect that the important part of the problem is happening near the tip, and this is where the points should be concentrated. The spacing that was typically used in numerical calculations was

$$\xi_i = \tan^2(\chi\, i/m), \quad i = 1, \ldots, m < n \tag{3.7}$$

where χ is chosen so that $\tan^2(\chi) = O(10)$, and the remaining points are added in a geometric progression, so that

$$\xi_{i+1} = (\xi_m/\xi_{m-1})\xi_i, \quad i = m, \ldots, n-1 \tag{3.8}$$

3.2. *Linear Perturbation Problem*

From equation 4.6b, we anticipate a singularity of the form ξ^{s-1} in $\tilde{H}'$, (we still expect a $\xi^{-1/2}$ singularity in $\tilde{G}'$). Therefore, the interpolation was changed to reflect this. Some of the integrals no longer have exact expressions. In this case, they are calculated by a numerical integration routine.

The lubrication equation for the linear perturbation problem (4.5b), is linear in $\tilde{H}$. Therefore, we can obtain two expressions for $\tilde{\Pi}(\zeta_i)$ that are linear in $\tilde{G}'(\xi_j)$, $\tilde{H}'(\xi_j)$. Together with the boundary conditions and beam theory asymptotics, (we haven't changed the integral kernel, so the asymptotics remain the same) there are enough equations to numerically solve the linear perturbation problem. There is no need to use Newton's method, as we can simply solve the linear set of equations.

3.3. *Double Tip*

In solving the problem of two tips situated at $-L$ and 0, an additional r points are taken to cover $-L \leqslant \xi < 0$. The spacing of points for $\xi < 0$ was chosen so that there was a concentration of points near $-L$ and near 0.

We interpolate G' expecting a $\xi^{-1/2}$ singularity at $\xi = -L$, and H' expecting a $\xi^{-1/2}$ singularity at $\xi = 0$. We do not calculate Π for $\xi < 0$ (although it is easily done), but just require that $\sigma_{xy} = 0$ for $\xi < 0$. This provides enough equations for the problem to be solved as before, with Newton's method.

Note that we input $-L$ and λ and recover κ_I, κ_{II}, where κ_I is measured at 0. From this, we extrapolate to $\kappa_I = 0$, and invert the relations so that $\lambda = \lambda(\kappa_{II})$, $L = L(\kappa_{II})$, to reflect the physical interpretation.

4. Results

4.1. *Single tip*

The single problem was solved numerically for the full range of λ values, $0 \leqslant \lambda < 0.059$, which corresponds to the values $0 < \kappa_I \leqslant 1.9$. In this section, we arbitrarily chose κ_I to be the parameter determining the speed, although it would have been equally valid to consider κ_{II} as the independent parameter. The results for H, G, and Π are shown in figure 2, along with the predicted asymptotics. The numerical solutions correspond well with the expected behaviour both as $\xi \to 0$ and $\xi \to \infty$.

It is then of interest to ask how κ_I, κ_{II} and λ are related in this model. When $\lambda = 0$ the problem becomes a static one, that should not depend on the fluid. The static problem of a semi-infinite crack has been studied by Thouless et al. (1987), who found that $(\kappa_I, \kappa_{II}) = (1.934, 1.503)$, which agrees with our numerical result to within the degree of accuracy, to which the values were given (0.2%). A plot of κ_I, λ, is shown in figure 3. A notable feature is how $\kappa_I \to 0$ as $\lambda \to 0.059$, with $\mathrm{d}\kappa_I/\mathrm{d}\lambda \to -\infty$. We will explain this

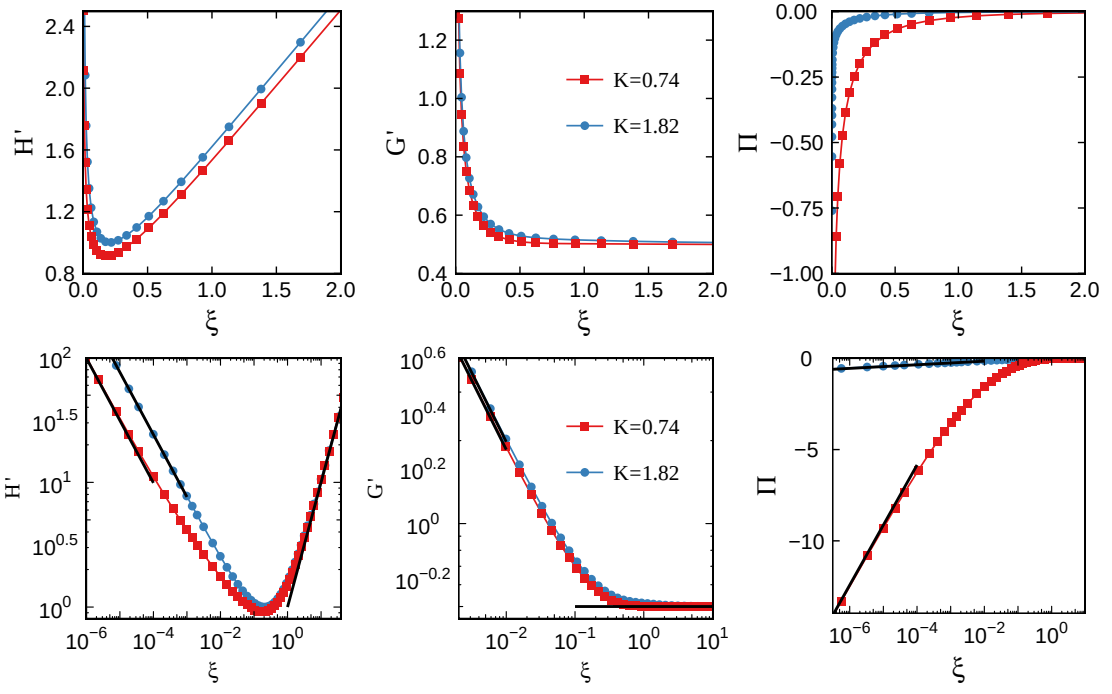

FIGURE 2. Numerical solutions for two typical values of κ_I. Logarithmic scales are shown, with solid lines indicating the predicted asymptotics; $H' \sim \kappa_I \xi^{-1/2}/(3\sqrt{2\pi})$, $G' \sim \kappa_{II}\xi^{-1/2}/(3\sqrt{2\pi})$, $\Pi \sim 9\pi\lambda/(2\kappa_I^2)\,\ln(\xi)$, as $\xi \to 0$, and $H' \sim \xi$, $G' \to 1/2$, $\Pi \to 0$ as $\xi \to \infty$. Figure produced with $n = 465$, $\xi_n = 819$.

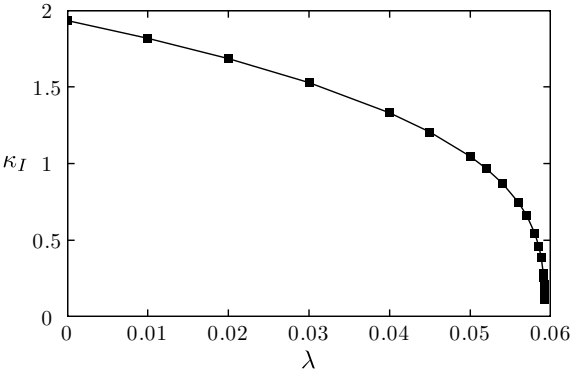

FIGURE 3. Here we vary the parameter λ and plot the change in κ_I. Figure produced with $n = 465$, $\xi_n = 819$.

behaviour by perturbing the $\kappa_I = 0$ solution and showing that the problem reduces to one studied by Garagash & Detournay (2005).

4.1.1. *Small toughness solution*

Consider the system with $\kappa_I = 0$, the zero toughness solution. In particular, consider the region $\xi \ll 1$, so zoomed in on the crack tip. Here, the problem should reduce to one of a semi-infinite crack in an unbounded domain. In this geometry, the elasticity integral

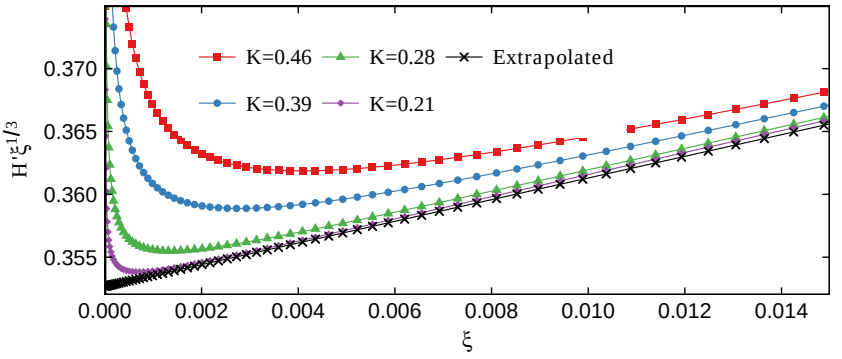

FIGURE 4. As $\kappa_I \to 0$, H' moves from a $\xi^{-1/2}$ singularity to a $\xi^{-1/3}$ singularity. We can not calculate H' for $\kappa_I = 0$, but the extrapolation to it is shown. Figure produced with $n = 465$, $\xi_n = 819$.

reduces to a much simplified form,

$$\Pi(\xi) = \int_0^\infty \frac{h'(\tilde{\xi})}{\tilde{\xi} - \xi} \mathrm{d}\tilde{\xi}. \tag{4.1}$$

From these reduced equations, one can find the leading order behaviour of the variables,

$$H_0 = A_0 \xi^{2/3} + o(\xi^{2/3}), \quad G_0 = B\xi^{1/2} + o(\xi^{1/2}), \quad \Pi_0 = \frac{3\lambda_0}{A_0^2 \xi^{1/3}} + o(\xi^{-1/3}) \quad (4.1a, b, c)$$

But this presents a problem; for any small $\kappa_I > 0$, $H \sim \xi^{1/2}$ near $\xi = 0$, which is incompatible with the $\kappa_I = 0$ behaviour. This is resolved by a boundary layer, where the solution looks like the $\kappa_I = 0$ almost everywhere except in a thin region near the crack tip.

Evidence for a boundary layer is shown in figure 4, as κ_I decreases, the behaviour of H' changes from $H' \sim \xi^{-1/2}$ to looking more like $H' \sim \xi^{-1/3}$, except in a thin region near $\xi = 0$.

Since this boundary layer is confined to a small region near the crack tip, and the appearance of some small κ_I shouldn't effect the solution away from the boundary layer, it is therefore important to understand what is happening right at the crack tip, so we consider again the simpler problem of a semi-infinite crack in an unbounded domain. This shape of crack, filled with an incompressible fluid, has been studied by Garagash & Detournay (2005). In particular they considered the situation in which a the solid had a small κ_I value, the small toughness solution.

They find that for $\kappa_I \ll 1$, there is a boundary layer of size $O(\kappa_I^6)$. Outside this layer, we expect to find corrections to the zero toughness solutions of the form

$$\begin{aligned} H(\xi) &= H_0(\xi) + \mathcal{E}(\kappa_I) H_1(\xi) + \dots \\ G(\xi) &= G_0(\xi) + \mathcal{E}(\kappa_I) G_1(\xi) + \dots \\ \Pi(\xi) &= \Pi_0(\xi) + \mathcal{E}(\kappa_I) \Pi_1(\xi) + \dots \\ \lambda &= \lambda_0 + \mathcal{E}(\kappa_I) \lambda_1 + \dots, \end{aligned} \tag{4.2}$$

where $\mathcal{E}(\kappa_I) = C\kappa_I^u \lambda_0^{2s-1}$. The numbers $s \approx 0.139$, and $u = 4 - 6s \approx 3.168$ come from solving a transcendental equation, and C must be determined numerically. Figure 5 shows remarkably good agreement with the prediction $\lambda \approx \lambda_0 + C\lambda_1 \kappa_I^u$, even for relatively large κ_I.

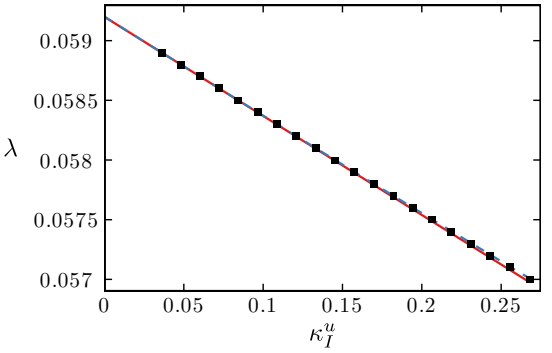

FIGURE 5. The numerical values of κ_I^u are plotted as points against the values of λ. A linear fit from the two smallest κ_I values is plotted as a solid line, a quadratic fit from the three smallest κ_I values is plotted as a dashed line. They are almost indistiguishable at this scale. The difference between the two extrapolations to $\kappa_I = 0$, provides an estimate of the error in calculating λ_0, (not accounting for the error due to n), which in this instance is $\approx 0.002\%$. This figure was made with $n = 524$, $\xi_n = 846$.

Garagash and Detournay calculate (after appropriate rescaling) $C = 3.488 \times 10^{-5}$. In order to determine C, and not $C\lambda_0^{2s-1}\lambda_1$, we solve a linearised problem for H_1, and calculate λ_1 from that.

4.1.2. *Calculating H_0*

$H(\xi;\kappa_I = 0) = H_0$ will be needed in order to find H_1 and λ_1. Numerically, for each ξ_i, $H'(\xi_i;\kappa_I = 0)$ is extrapolated from $H'(\xi_i,\kappa_j)$ from two κ_j values. Figure 4 shows that $H'(\xi;0.21)$ is a good approximation to $H'(\xi;0)$, away from a boundary layer near $\xi = 0$. The size of the boundary layer becomes smaller as κ_I decreases, but to avoid using very small values of κ_I, the effects of the boundary layer are removed by simply extending the linear trend present in $0.002 < \xi < 0.003$ all the way to $\xi = 0$.

4.2. *Linear perturbation problem*

Supposing one has found H_0 numerically, or otherwise. Substituting the expansion for H, Π, into the equations and keeping only terms of order $\mathcal{E}$, gives the relations

$$\begin{bmatrix} \Pi_1 \\ 0 \end{bmatrix} = \int_0^\infty \boldsymbol{K}(\xi - \tilde{\xi}) \begin{bmatrix} G_1'(\tilde{\xi}) \\ H_1'(\tilde{\xi}) \end{bmatrix} \mathrm{d}\tilde{\xi}, \qquad H_0^2\Pi_1' + 2H_0H_1\Pi_0' = \lambda_1 \tag{4.3a, b}$$

$$H_1'' \to 0 \text{ as } \xi \to \infty, \qquad H_1 \sim \xi^s + \frac{\tilde{A}\lambda_1}{3\lambda_0^{2/3}}\xi^{2/3} + \dots \text{ as } \xi \to 0. \tag{4.4a, b}$$

But these can be made into a more convenient form, by considering instead $\tilde{\Pi} = \Pi_0 - 3\lambda_0/\lambda_1\Pi_1$, and similar for $\tilde{H}$, $\tilde{G}$. The equations become

$$\begin{bmatrix} \tilde{\Pi} \\ 0 \end{bmatrix} = \int_0^\infty \boldsymbol{K}(\xi - \tilde{\xi}) \begin{bmatrix} \tilde{G}'(\tilde{\xi}) \\ \tilde{H}'(\tilde{\xi}) \end{bmatrix} \mathrm{d}\tilde{\xi}, \qquad H_0^2\tilde{\Pi}' + 2H_0\tilde{H}\Pi_0' = 0 \tag{4.5a, b}$$

$$\tilde{H}'' \to 1 \text{ as } \xi \to \infty, \qquad \tilde{H} \sim -\frac{3\lambda_0}{\lambda_1}\xi^s + \dots \text{ as } \xi \to 0 \tag{4.6a, b}$$

These equations were solved numerically, the results are plotted in figure 6. The figure shows that the $\tilde{H}$ behaves like ξ^s near the origin. However, it is very difficult to get reliable numerical estimates of the intercept. This is partly due to the difficulty in calculating H_0

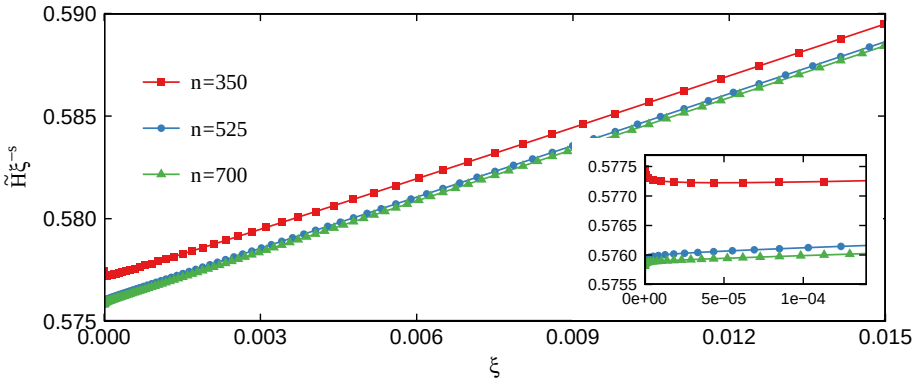

FIGURE 6. The numerical solution of the linear perturbation problem near $\xi = 0$ for a selection of resolutions, all with $\xi_n = 875$. Of interest, is the value of the intercept, which as shown is dependent on the resolution. Also shown is the numerical divergence near the tip, due to the difficulty in calculating H_0 for $\xi \ll 1$.

and removing the boundary layer present in $H(\xi;\kappa_I)$ solutions, as well as dependance on n, ξ_n. Our best guess would be that $-3\lambda_0/\lambda_1 \approx 0.58$. Figure 5 gives $\lambda_0 \approx 0.059$, $C\lambda_1\lambda_0^{2s-1} \approx 8.3 \times 10^{-3}$, which in total gives our calculation of $C \approx 3.5 \times 10^{-3}$, in agreement with the value in Garagash and Detournay.

4.3. *Two tips*

After the linear perturbation problem, we move on to the two tip problem. Perhaps some graphs that show an outline of the full numerical problem with non-zero κ_I and κ_{II}, although these are not physical.

We now move on to the $\kappa_I = 0$ set of relations.

Approximate formula in the single tip case:

$$\lambda \approx 0.059 - 0.0083\kappa_I^u + 0.00033\kappa_I^{3u/2} \tag{4.7}$$

$$\lambda \approx -1.5 + 2.7\kappa_{II} - 1.1\kappa_{II}^2 \tag{4.8}$$

In the double tip case:

$$\lambda \approx 0.10 - 0.022\kappa_{II}^2 \tag{4.9}$$

These equations provide a fairly good approximation to the data, see figure 10.

From dry fracture mechanics and conservation of energy, one expects a relationship of the form $\lambda = \alpha + \beta\kappa_{II}^2$. However, in this case, α and β should depend on the geometry, H, and so should be functions of κ_{II}. However, numerical evidence shows them as being approximately constant. Part of the reason for this, is the decoupling between the fluid problem and the dry tip. Suppose one solves the two tip problem, for some L. This gives a geometry, the reference H'. From this, one can choose any λ, and find G', and value of κ_{II}. The effect of this is shown in figure 11, a changing H' has little effect on the λ, κ_{II} relationship.

5. Discussion

Acknowledgements should be included at the end of the paper, before the References section or any appendicies, and should be a separate paragraph without a heading. Several anonymous individuals are thanked for contributions to these instructions.

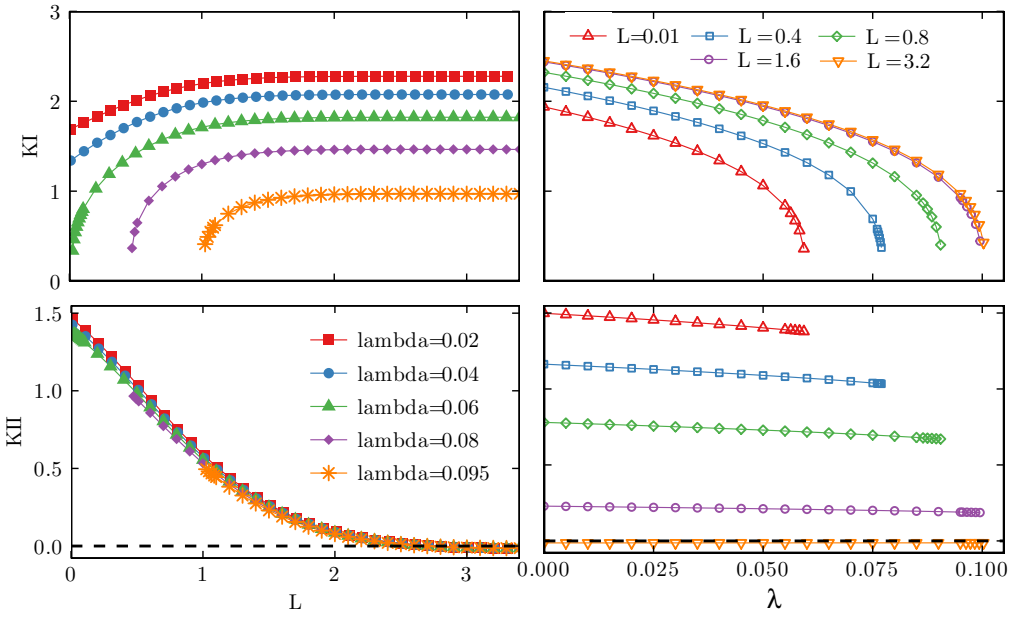

FIGURE 7. Some of the numerical results for the two tip problem. Having $\kappa_I \neq 0$ at $\xi = 0$ and $L \neq 0$ is unphysical, but is what is found numerically. We can recover the physical solution by increasing λ for fixed L until $\kappa_I = 0$. Figure made with $n = 995$, $\xi_n = 846$.

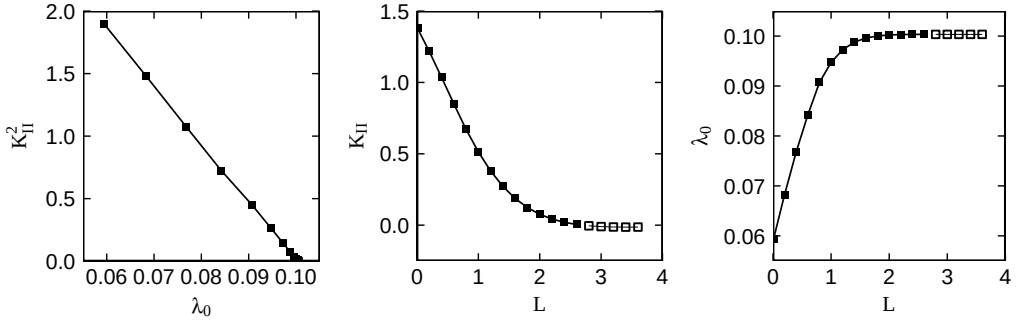

FIGURE 8. The results of extrapolating to $\kappa_I = 0$. Hollow squares indicate a value of $\kappa_{II} < 0$. Figure made with $n = 995$, $\xi_n = 846$.

REFERENCES

DYSKIN, A. V., GERMANOVICH, L. N. & USTINOV, K. B. 2000 Asymptotic analysis of crack interaction with free boundary. *Intl. J. Solids and Structures* **37**, 857–886.

THOULESS, M. D., EVANS, A. G., ASHBY, M. F., & HUTCHINSON, J. W. 1987 The edge cracking and spalling of brittle plates. *Acta metall.* **35**, 1333–1341.

GARAGASH, D. I & DETOURNAY, E. 2005 Plane-strain propagation of a fluid-driven fracture: small toughness solution. *J. Appl. Mech.* **72**, 916–928.

ZLATIN, A. H. & KHRAPKOV, A.A. 1986 A Semi-Infinite Crack Parallel to the Boundary of the Elastic Half-Plane. *Dokl. Akad. Nauk SSSR.* **31**, 1009-1010.

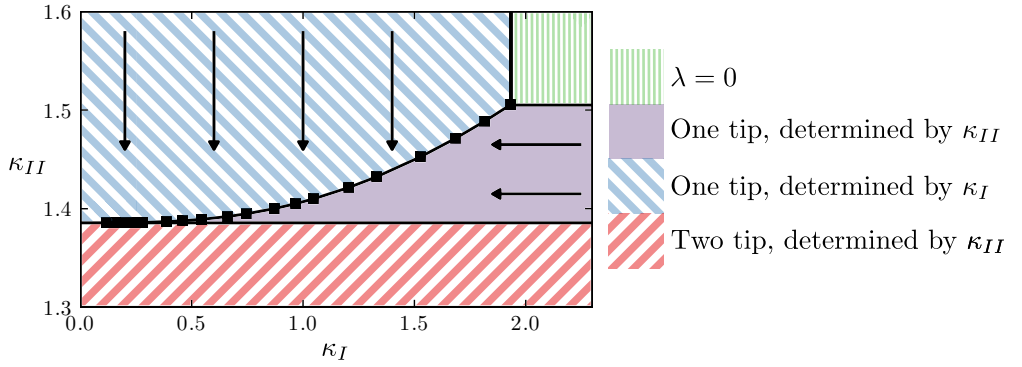

FIGURE 9. Given values (κ_I, κ_{II}), this graph determines which frature regime occurs and so how λ and/or L should be calculated. Figure made with $n = 465$, $\xi_n = 819$.

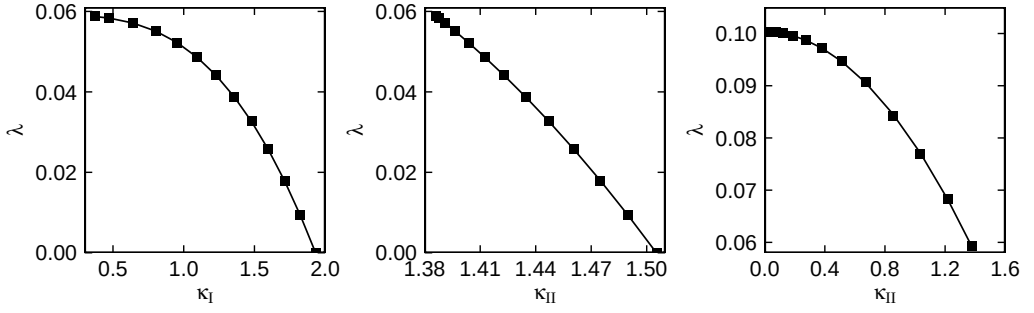

FIGURE 10. The formula (solid lines) giving good approximation to the calculated values (symbols). For the single tip calculations, $n = 815$ was used, for the double tip $n = 995$. $\xi_n = 846$ in both cases.

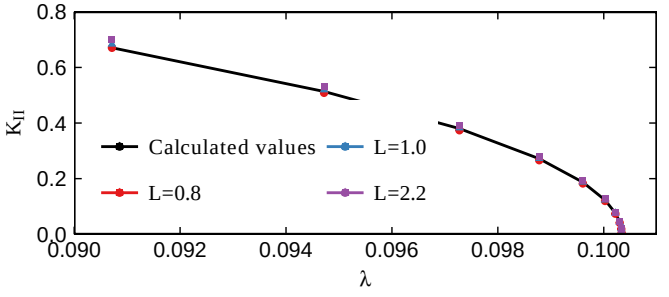

FIGURE 11. Reconstructing the full solution given a reference H'. Figure made with $n = 995$, $\xi_n = 846$.